

# SCIENTIFIC REPORTS



OPEN

## Periodic fluctuation of reference evapotranspiration during the past five decades: Does Evaporation Paradox really exist in China?

Received: 24 August 2016  
Accepted: 23 November 2016  
Published: 19 December 2016

Wanqiu Xing<sup>1,2</sup>, Weiguang Wang<sup>1,2</sup>, Quanxi Shao<sup>3</sup>, Zhongbo Yu<sup>1</sup>, Tao Yang<sup>1,2</sup> & Jianyu Fu<sup>1,2</sup>

Evidence that the pan evaporation or reference evapotranspiration ( $ET_0$ ) as the indicator of atmospheric evaporation capability have decreased along with the continuous increase in temperature over the past decades (coined as “evaporation paradox”) has been reported worldwide. Here, we provide a nationwide investigation of spatiotemporal change of  $ET_0$  using meteorological data from 602 stations with the updated data (1961–2011). In addition, we explore the trigger mechanism by quantitative assessment on the contribution of climatic factors to  $ET_0$  change based on a differential equation method. In despite of different shift points regionally, our results suggest that the  $ET_0$  generally present decadal variations rather than monotonic response to climate change reported in previous studies. The significant decrease in net radiation dominate the decrease in  $ET_0$  before early 1990s in southern regions, while observed near-surface wind speed is the primary contributor to the variations of  $ET_0$  for the rest regions during the same periods. The enhancements of atmospheric evaporation capability after early 1990s are driven primarily by recent relative humidity limitation in China. From a continental scale view, as highly correlating with to Pacific Decadal Oscillation, the shift behaviors of  $ET_0$  is likely an episodic phenomenon of the ocean-atmosphere interaction in earth.

As the only connecting term between water and energy balance, evapotranspiration is the best indicator for the response behavior of transport of water vapor and latent heat as well as hydrological course and the terrestrial ecosystems associated with climate change<sup>1,2</sup>. Along with significantly increasing near-surface air temperatures, decreasing pan evaporation ( $ET_{pan}$ ), potential evapotranspiration ( $ET_p$ ) and reference evapotranspiration ( $ET_0$ ) have been reported in many regions worldwide and continuously documented by many studies since the first publication by Peterson *et al.* in 1995<sup>3</sup>. This phenomenon has been denoted as the “evaporation paradox”<sup>4</sup>. However, the interpretations for this phenomenon by different scholars are various in different regions, mainly including the following: (1) decreasing  $ET_p$  or  $ET_0$  may actually be a strong indication of increasing terrestrial evaporation due to the complementary relationship between the actual evaporation and potential evaporation<sup>5–9</sup>; (2) positive effect on evapotranspiration of increasing temperature could be offset by widespread “dimming” and “stilling” phenomena due to the fact that evaporative process is also primarily driven by radiative and aerodynamic components<sup>4,10,11</sup>.

Decreases in  $ET_p$ ,  $ET_{pan}$ , and  $ET_0$  have also been reported to be occurring simultaneously in China or some regions of China with increasing trends of air temperature during the past decades<sup>12–19</sup>. Reduced wind speed and shortened sunshine duration are generally considered to be responsible for these phenomena<sup>9,20–22</sup>. However, some of conclusions drawn from previous studies on evapotranspiration trends are based on the time series data ended around 2000. Whether the decreasing trends in potential evaporation are still true when looking at the longer record with updated data should also be addressed. In addition, most studies mainly focus on the general trends without the consideration of the abrupt change in the temporal processes. Overall trend estimations may leave out detailed information and thus make these revealed changing patterns deviate from the real situation. Recently, contrary to the famous “evaporation paradox”, an increase in  $ET_{pan}$  in China along with continuously

<sup>1</sup>State Key Laboratory of Hydrology-Water Resources and Hydraulic Engineering, Hohai University, Nanjing 210098, China. <sup>2</sup>College of Water Resources and Hydrology, Hohai University, Nanjing 210098, China. <sup>3</sup>CSIRO Data 61, Private Bag 5, Wembley, WA 6913, Australia. Correspondence and requests for materials should be addressed to W.W. (email: wangweiguang006@126.com)

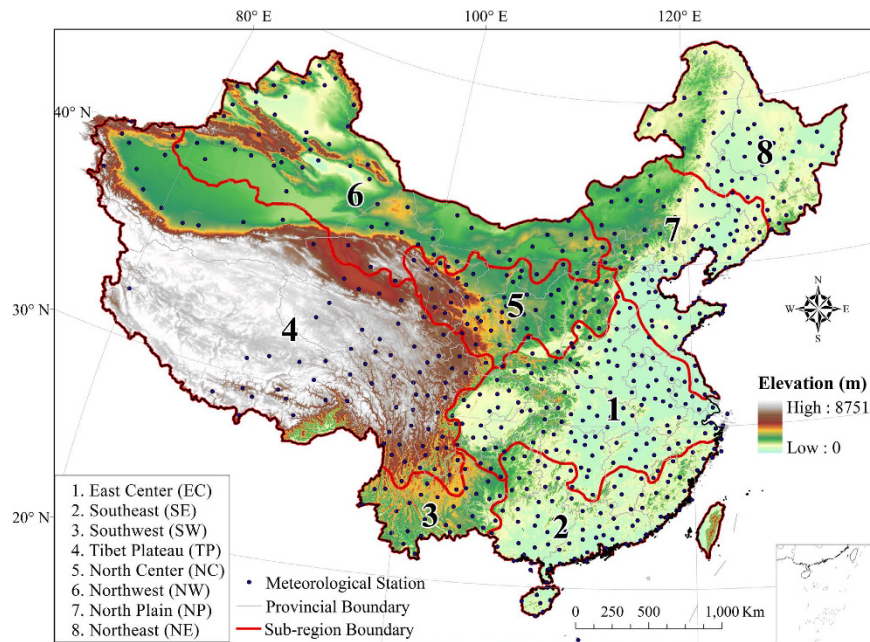


**Figure 1. The sub-regions identified by REOF analysis and the spatial distribution of 602 meteorological stations in Mainland China.** This figure was created using the ArcGIS 9.3 (<http://www.esri.com/software/arcgis/arcgis-for-desktop>).

rising temperature during the recent two decades was identified by Liu *et al.*<sup>23</sup> with more recent observations. This phenomenon was further regionally verified in the hyper-arid region of Northwest of China by Li *et al.*<sup>24</sup>. Moreover, Wang *et al.*<sup>25</sup> suggested that there was actually a zigzag increasing–decreasing–increasing pattern of regional average  $ET_0$  series with two joint points in 1973 and 1993 in the Tibetan Plateau. It is therefore worthwhile to re-examine the  $ET_0$  patterns in larger area with different climatic and geomorphologic conditions based on the updated data. However, nationwide investigation on the changing patterns of  $ET_0$  and its related trigger mechanism is not available.

The goal of this study is to examine whether the “evaporation paradox” is still true by investigating the response of  $ET_0$  to changing climatic environment based on recently updated nationwide observation in China. Specifically, we begin by identifying the homogeneously sensitive regions of  $ET_0$  using a rotated empirical orthogonal function clustering method. Then we assess the spatial patterns of  $ET_0$  trends and analyze the abrupt change in average series for individual homogenous regions. Meanwhile, special efforts are further made in characterizing the underlying aerodynamic and radiative driving mechanism for the  $ET_0$  changes. Finally, the driving mechanisms under natural large atmosphere system are explored by identifying the correlation between changes in  $ET_0$  and Pacific Decadal Oscillation.

## Results

**Identification of homogenous regions of  $ET_0$ .** To intensively characterize the spatial anomalies of  $ET_0$  change nationwide, it is necessary to make a reasonable partition to the whole country. Traditionally, the whole China is always divided into eight climatic regions according to the latitude and longitude, and the climate regions are roughly coincide with the socioeconomic division<sup>13,23</sup>. However, there may be some uncertainty in sub-region selection based on visual inspection of the geographical distribution or administrative practices due to its vulnerability to subjective discretion<sup>9</sup>. This is especially true for the study of  $ET_0$  changing patterns due to the fact that  $ET_0$  involve in multifarious factors including geomorphologic features, topography factors and climate conditions. Therefore, the rotated empirical orthogonal function (REOF) method, a widely used clustering algorithm to objectively capture realistic spatial information, is employed in the current study to identify the homogenous regions regarding  $ET_0$  in the whole China. The first 11 EOFs together explain 80.8% of the variance and the first 8 EOFs together can explain 73.7% of the variance. The fact that more than 70% of the total variability is captured in the first 8 EOFs indicates that the complexity of spatial patterns of  $ET_0$  all over the country can mostly be explained by a small number of spatial structures. The percentages of variance of the new set of REOF modes generated by rotating the first eight loading vectors of the initial EOFs (Table S1) and correspondent isolines of the loading factor values (Figure S1) suggest that Mainland China can be categorized into eight homogenous regions (Fig. 1) by REOF analysis based on the annual  $ET_0$  series from 602 stations for 1961–2011. Eight leading modes deduced sub-regions can roughly be described respectively as following: East Center China (EC), Southeast China (SE), Southwest China (SW), Tibet Plateau (TP), North Center China (NC), Northwest China (NW), North China Plain (NP), and Northeast China (NE). In term of the regional average series of these eight homogenous regions, investigation on temporal patterns and their attributions across the whole China are presented in following sections.

**Multidecadal changing patterns in  $ET_0$ .** We conduct trends and change point analysis for the area-averaged  $ET_0$  in the resulted eight sub-regions by the means of the segmented regression model (shown in Fig. 2 and Table 1). The overall impression from the temporal patterns in  $ET_0$  series is that shift trends can be evidently found in all eight sub-regions, although the turning years and the number of change points are regionally different. The decreasing-increasing (DI) patterns (with one joint point) are detected in EC, SE and SW regions with joint points happening at about 1992, 1992 and 1995, respectively. The zigzag increasing-decreasing-increasing (IDI) patterns (with two joint points) are depicted in TP (1973 and 1993) and NW (1977 and 1995) regions. With three joint points, approximating to periodic variation, more complex zigzag increasing-decreasing-increasing-decreasing (IDID) patterns are identified in NC (1973, 1991 and 2000) and NE (1978, 1993 and 2003) regions. It should be noted that although only two points of 1992 and 2002 are found in NP region, the overall changing pattern of decreasing-increasing-decreasing for  $ET_0$  are similar to NC and NE regions, especially for the recent two decades. Interestingly, irrespective of complex shift trends reflected by different number of joint points and turning modes, multidecadal changing features in  $ET_0$  are characterized by an evident spatial clustering partition. This clustering partition can roughly indicates that DI patterns mainly occur in southern region in China with a humid climate, whereas IDI mostly emerge in western Plateau regions with a cold and drought climate and IDID mainly appear in north and northeast regions with a cold climate. We also investigate the trends for the 602 stations during the segmented periods according to the corresponding regional change points. Taking EC region for example, as shown in Fig. 3, annual  $ET_0$  at all stations decrease during 1961–1991 by  $0–8 \text{ mm yr}^{-1}$  (over 23% stations by  $4–8 \text{ mm yr}^{-1}$ ), of which over 80% stations are statistically significant at 95% confidence level ( $p < 0.05$ ). As for as the second segmented period, from 1992–2011, more than 65% stations (over 30% stations by  $4–12 \text{ mm yr}^{-1}$ ) are dominated by increasing trends in  $ET_0$  despite that only 35% stations are statistically significant at 95% confidence level ( $p < 0.05$ ). Such extremely distinct spatial patterns in  $ET_0$  during the adjacent segmented period are also identified in other homogeneous regions (shown in Figure S2–S8), giving us confidence in detecting multidecadal changes in  $ET_0$  with shift trends in China.

**Driving factors of changing  $ET_0$ .** The “evaporation paradox” is stated based on measured pan evaporation<sup>3</sup>, therefore, the correlation analyses of  $ET_0$  with  $ET_{\text{pan}}$  (data collected from 183 stations with the same records of  $ET_0$ ) is conducted before the contribution assessment of climatic factors. The close relationship between annual  $ET_{\text{pan}}$  and  $ET_0$  with correlation coefficient ( $R$ ) of more than 0.9 suggests that  $ET_{\text{pan}}$  is a good indicator of  $ET_0$  across the whole China (Figure S9). We identify the driving factors of changing  $ET_0$  by quantifying the contribution of climatic factors to  $ET_0$  change using partial derivatives (see Equation 10). For the eight homogeneous regions, the maximum relative error  $\rho(\delta)$  representing the ratio of error  $\delta$  to observed trend is found in NC region during the fourth segmented period of 2000–2011 with the value of  $-14.78\%$ . The minimum  $\rho(\delta)$  is only 1.70%, which occurs in NP region during the first segmented period of 1961–1991 (Table S2). The calculated  $ET_0$  trends for all regions during all the segmented periods match very well with those detected from the computed  $ET_0$  with P-M method (always regarded as observed ones) with quite satisfactory  $R^2$  value of 0.99. The high accordance of calculated  $ET_0$  trends with estimated ones reflected by high  $R^2$  and low error indicates the differential equation method is applicable to quantify the contributions of climatic variables to changes in  $ET_0$ . The contributions of climatic factors to the trends in  $ET_0$  in categorized eight sub-regions during different periods are shown in Fig. 4. Taking NC regions with most complex shift trends in  $ET_0$  as an example, during 1961–1972, the decreasing air temperature ( $T$ ) causes a decrease of  $ET_0$  at the rate of  $0.42 \text{ mm yr}^{-1}$ . Meanwhile, the increase of wind speed ( $U$ ) and net radiation ( $R_n$ ) as well as the decrease of relative humidity ( $RH$ ) lead to the increase of  $ET_0$  at the rate of  $2.53 \text{ mm yr}^{-1}$ ,  $0.85 \text{ mm yr}^{-1}$  and  $1.18 \text{ mm yr}^{-1}$ , respectively. Consequently,  $U$  is the dominant factor for the change in  $ET_0$  in NC region during 1961–1972. Likewise,  $U$ ,  $RH$  and  $R_n$  are responsible for the decrease of  $ET_0$  during 1973–1990, the increase of  $ET_0$  during 1991–1999 and the decrease of  $ET_0$  during 2000–2011 in NC region, respectively. Overall, although the change in  $ET_0$  of the whole country is characterized by complicated spatial and temporal variability in the dominating contribution factors, some interesting phenomena can be summarized as below. Before the early 1990s, the decreases of  $ET_0$  in EC, SE and SW regions, mostly located in South China, are mainly attributed to the decrease of  $R_n$ . While for the rest regions including TP, NC, NW, NP and NE, mainly distributed in western and northern part of China, the changes of  $ET_0$  before the early 1990s (all consist of increasing period before 1970s and subsequent decreasing period except NP region) mainly resulted from the changes of  $U$ , except the NE region during 1961–1977 with the dominating factor  $RH$ . From early 1990s to 2011, the  $ET_0$  in EC, SE, SW, TP and NW regions present monotonous increase. While for the NC, NP and NE regions, changes in  $ET_0$  are separated into two stages, i.e., increases from early 1990s to around 2000 and decreases after 2000. Although  $R_n$ ,  $T$  and  $U$  play respectively the most import role in the decrease of  $ET_0$  at NC, NP and NE regions after around 2000, decreasing trends in  $RH$  is the most crucial factor for the increasing trends in  $ET_0$  detected after the early 1990s in all the eight sub-regions.

**The linkage between multidecadal patterns of  $ET_0$  and the Pacific Decadal Oscillation (PDO).** In order to investigate the decadal characteristic of  $ET_0$  in China and seek for the possible driving mechanisms, the regional mean anomalies of annual  $ET_0$ , precipitation ( $P$ ) and the climatic water availability (CWD, defined as  $P$  minus  $ET_0$ ) as well as its relationship to the Pacific Decadal Oscillation index (PDO) are analyzed. Although as a whole, the regional  $ET_0$  record shows a significant decrease trend of  $0.298 \text{ mm yr}^{-2}$  ( $p < 0.1$ ) during the past 50-years period, the evolving process of continental mean  $ET_0$  can be clearly divided into three stages. From 1961 to 1979,  $ET_0$  present a slight but not significant decline ( $0.008 \text{ mm yr}^{-2}$ ) with a high mean value. A prolonged significant decline starts in the year of 1980 and ends in the year of 1995, being contrary to the previously reported upward actual evapotranspiration in this period<sup>26–28</sup>. This may partly be explained by the complementary relationship<sup>29</sup> between  $ET_0$  and actual evapotranspiration. After 1996, a pronounced recovery growth rate in  $ET_0$  can be clearly revealed. An overall oscillation in regional mean  $ET_0$  is found in China, which

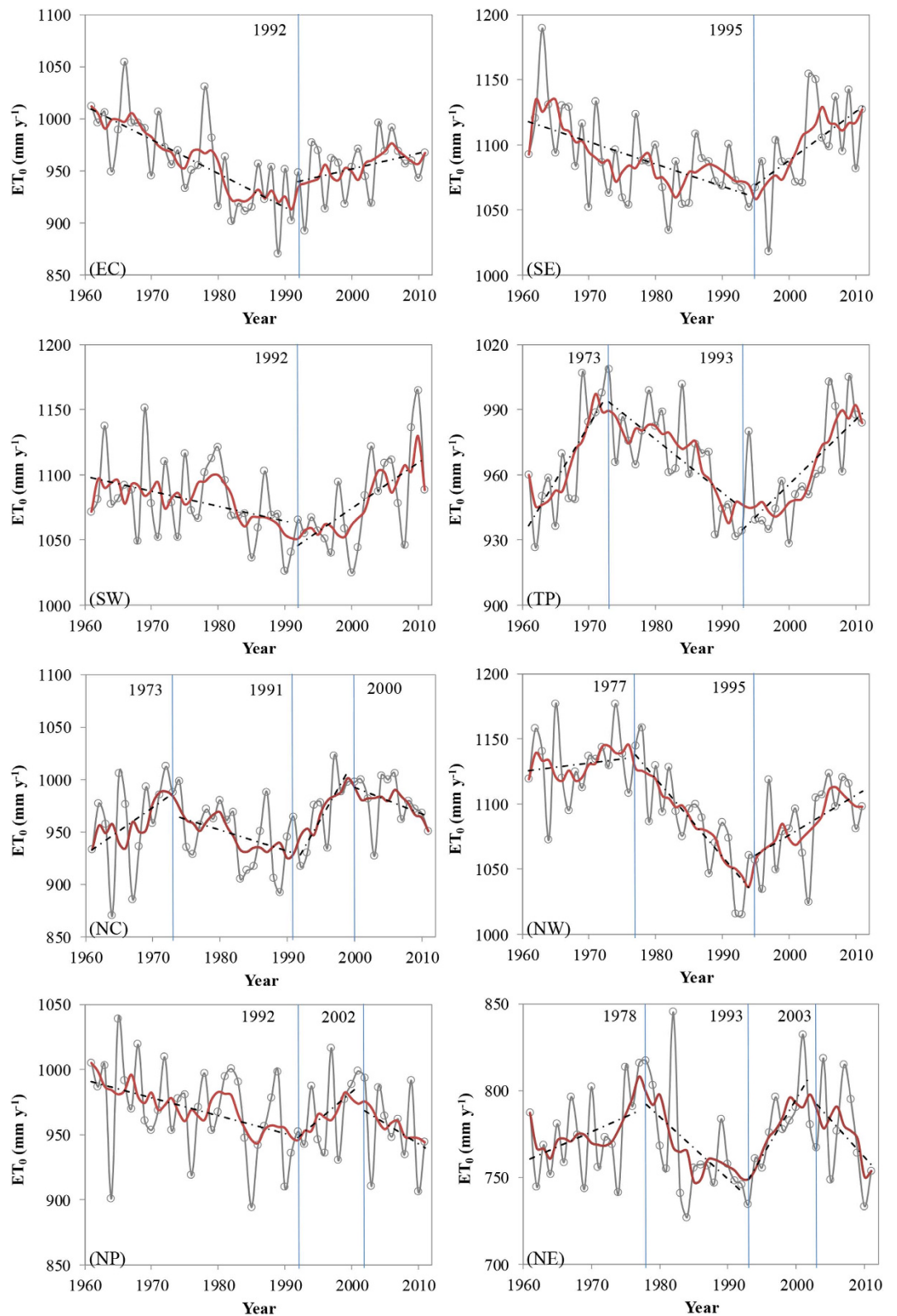


**Figure 2.** Long term variations and abrupt change of annual reference evapotranspiration ( $ET_0$ ) for the eight subregions during 1961–2011. The grey solid line with circles and the red line denotes the observed series and the smoothed series, respectively. The blue vertical line give the location of change points and the black dash lines are the segmented linear trends fitted to corresponding periods.

Sub-region	Variables	Trend Slope		Sub-region	Variables	Trend Slope				
EC	Periods		1961–1991	1992–2011	NC	Periods	1961–1972	1973–1990	1991–1999	2000–2011
	$ET_0$		-3.2646**	1.5064		$ET_0$	4.4246	-3.0376**	8.187*	-2.538
	$T$		-0.0048	0.0335**		$T$	-0.0142	0.0233	0.1705**	0.0185
	$RH$		0.0342	-0.2420**		$RH$	-0.1565	0.0474	-0.3429	-0.0562
	$U$		-0.0185**	-0.0113**		$U$	0.0355**	-0.0286**	0.0056	-0.0041
	$R_n$		-0.0194**	-0.0084		$R_n$	0.005	-0.0087	0.0087	-0.0225**
	Dominating Factor		$R_n$	$RH$		Dominating Factor	$U$	$U$	$RH$	$R_n$
SE	Periods		1961–1994	1995–2011	NW	Periods	1961–1976	1977–1994	1995–2011	
	$ET_0$		-1.7178**	3.7568**		$ET_0$	0.673	-5.9695**	3.0873**	
	$T$		0.0069	0.014		$T$	-0.0338	0.0275	0.0234	
	$RH$		-0.006	-0.3195**		$RH$	-0.0336	0.1075*	-0.1129	
	$U$		-0.0113**	-0.0032		$U$	0.0210**	-0.0402**	0.0055**	
	$R_n$		-0.0162**	0.0026		$R_n$	-0.001	-0.0044*	-0.0035*	
	Dominating Factor		$R_n$	$RH$		Dominating Factor	$U$	$U$	$RH$	
SW	Periods		1961–1991	1992–2011	NP	Periods		1961–1991	1992–2001	2002–2011
	$ET_0$		-1.1510**	3.5493**		$ET_0$		-1.3780**	4.3713	-3.1608
	$T$		0.0110*	0.0253*		$T$		0.0183*	0.0571	-0.1057*
	$RH$		-0.0298	-0.1921**		$RH$		-0.0118	-0.0939	-0.0467
	$U$		-0.0002	0.0156**		$U$		-0.0177**	-0.0187**	-0.013
	$R_n$		-0.0131**	0.0027		$R_n$		-0.0084**	0.0137	-0.0047
	Dominating Factor		$R_n$	$RH$		Dominating Factor		$U$	$RH$	$T$
TP	Periods	1961–1972	1973–1992	1993–2011	NE	Periods	1961–1977	1978–1992	1993–2002	2003–2011
	$ET_0$	5.1585**	-2.4605**	2.9879**		$ET_0$	1.7502	-3.5712*	6.5942**	-4.3362
	$T$	0.0282	0.0084	0.0525**		$T$	-0.0026	0.0809**	-0.0166	-0.0938
	$RH$	-0.1289**	0.0393	-0.2910**		$RH$	-0.0295	0.0899	-0.1885	0.1567
	$U$	0.0497**	-0.0239**	0.0015		$U$	0.0034	-0.0381**	-0.002	-0.0273**
	$R_n$	0.0161**	-0.0052*	-0.0052		$R_n$	0.0046	-0.0089	0.0242*	0.0189
	Dominating Factor	$U$	$U$	$RH$		Dominating Factor	$RH$	$U$	$RH$	$U$

**Table 1. Trend slope of reference evapotranspiration ( $ET_0$ ) and meteorological variables in linear regression analysis, and the dominating factor result to  $ET_0$  change by attribution analysis.** Note: Trend slope of linear regression of  $ET_0$ ,  $T$ ,  $RH$ ,  $U$ , and  $R_n$  are expressed in  $\text{mm yr}^{-1}/\text{y}$ ,  $^\circ\text{C}/\text{y}$ ,  $\%/y$ ,  $\text{m s}^{-1}/\text{y}$ , and  $\text{W m}^{-2}/\text{y}$ , respectively, and “\*” represent significance at  $p = 0.10$ , “\*\*” represent significance at  $p = 0.05$ .

was not revealed by the previous studies, suggesting that the variation of  $ET_0$  from 1961 to 2011 should be a phenomenon of earth’s atmospheric circulation. PDO is considered as the important earth’s climatic driving power for the continental hydro-meteorology abnormality such as shift of dry/wet in Asia, especially in China<sup>30–33</sup>. The PDO driven climate oscillations impart clear influences to the regional  $ET_0$  in China as a whole, indicated by significant negative correlation between annual PDO index and annual mean  $ET_0$  ( $r = -0.384$ ;  $p < 0.001$ ). Years with high  $ET_0$  mostly coincide with PDO cold phase although  $ET_0$  responses to PDO may differ in different sub-regions in China. On the other hand, years with low  $ET_0$  correspond to PDO warm phase conditions (Fig. 5). The regional mean P in China present large temporal variability with a negative but not significant trend of  $0.257 \text{ mm yr}^{-2}$  ( $p = 0.564$ ) during 1961–2011, while the CWD present a significantly no trend although the slope is slightly positive with the value of  $0.041 \text{ mm yr}^{-2}$  ( $p = 0.938$ ), suggesting that there is a weak tendency to reduce the deficit between atmospheric moisture requirement and available water supply for evapotranspiration. Despite of the strong relationship between regional  $ET_0$  and PDO activities, the CWD is not significantly correlated with PDO ( $r = 0.164$ ,  $p > 0.1$ ) due to the weak relationship between P and PDO ( $r = 0.045$ ,  $p > 0.1$ ).

## Discussion

The “evaporation paradox”, reported in many regions of the world including China<sup>15</sup>, has drawn a considerable attention to explore the reason of the decreases in  $ET_{\text{pan}}$  and/or  $ET_0$  with increases in air temperature. However, with more recent observations or longer record, an increase in  $ET_{\text{pan}}$  and/or  $ET_0$  since 1980s or 1990s has been found in China or some regions of China<sup>23,24,34–36</sup>. Specially, a zigzag increasing-decreasing-increasing pattern with two joint points in 1973 and 1993 has been identified in our previous study on the changes in  $ET_0$  across the Tibetan Plateau<sup>25</sup>. However, the results from most previous studies on  $ET_0$  change and driving mechanism are only based on subjective sub-regions selection. Meanwhile, the natural large atmosphere system triggering mechanisms for  $ET_0$  change have not been investigated in previous studies. Consequently, a nationwide investigation in China is naturally performed in this study to detect the real multidecadal changing patterns of  $ET_0$  and the correlation with PDO with extended data from 1961 to 2011. The temporal patterns of  $ET_0$  in eight homogeneous regions identified by REOF evidently reveal that there is no monotonous decreasing trend in  $ET_0$  along with the continuously increasing temperature for the entire period (from 1961 to 2011), suggesting “paradox”

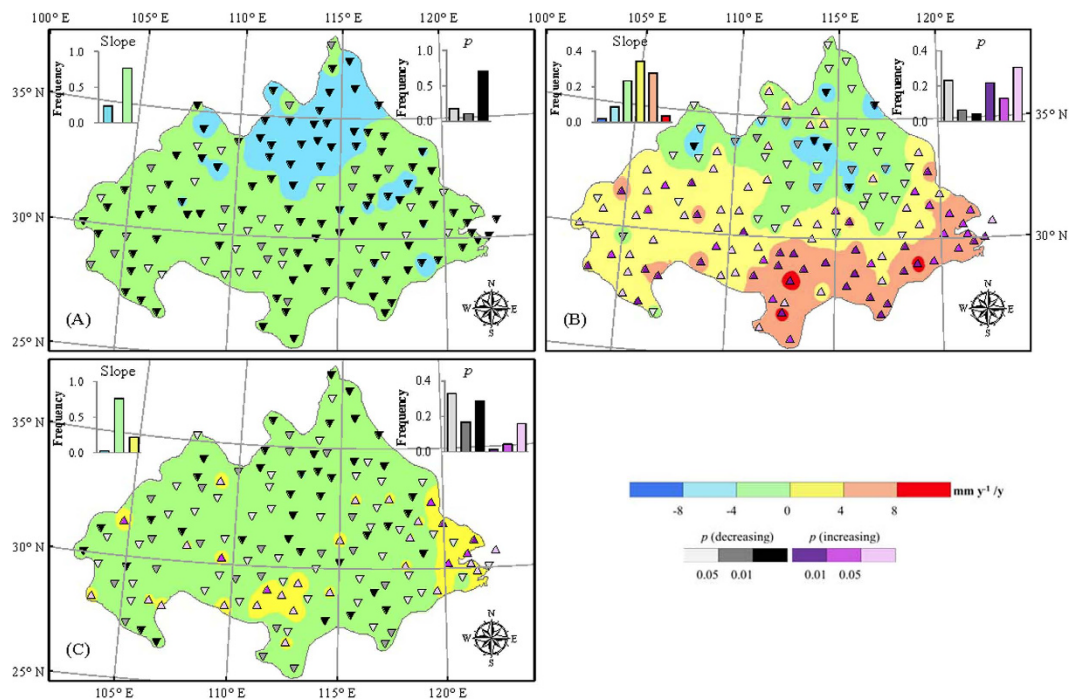


**Figure 3.** Spatial distributions of the change rate of reference evapotranspiration ( $ET_0$ ) and significance levels of the change in the first sub-region during the three periods ((A): 1961–1991; (B): 1992–2011; and (C): 1961–2011).  $p$ (decreasing) and  $p$ (increasing) are the  $p$  values of the decrease and increase in the annual reference evapotranspiration ( $ET_0$ ), respectively, which are divided into three levels:  $p < 0.01$ ,  $0.01 < p < 0.05$ , and  $p > 0.05$ . The insets show the frequency distributions of change trends of reference evapotranspiration ( $ET_0$ ) (left) and different significance levels (right). This figure was created using the ArcGIS 9.3 (<http://www.esri.com/software/arcgis/arcgis-for-desktop>).

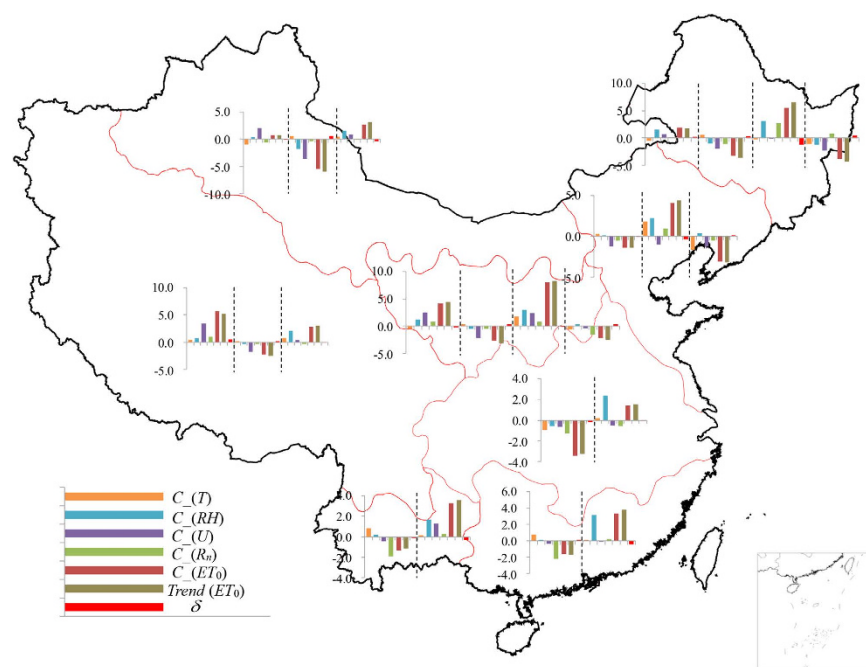


**Figure 4.** The contribution of annual climatic variables change to reference evapotranspiration ( $ET_0$ ) change in each sub-region. This figure was created using the ArcGIS 9.3 (<http://www.esri.com/software/arcgis/arcgis-for-desktop>).

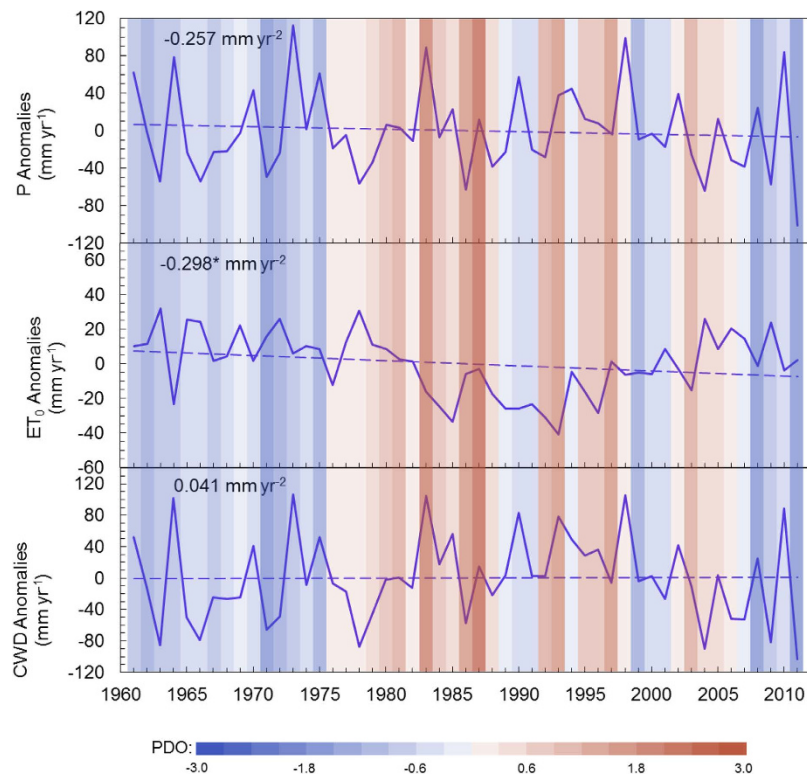


**Figure 5.** Yearly anomalies of P, reference evapotranspiration ( $ET_0$ ) and CWD ( $P - ET_0$ ) from 1961 to 2011; the linear trends of annual values of the three variables are calculated by the simple linear regression and shown as dashed lines, \* $p < 0.1$ , \*\* $p < 0.05$ . The Pacific Decadal Oscillation index, PDO, is shown with vertical color shading, where red and blue shades denote respective positive and negative phases.

phenomenon just exist in a certain stage of the multidecadal changes in  $ET_0$  in China. With one turning point, the finding that decreasing trends of  $ET_0$  reverse into increasing trends in early 1990s across EC, SE and SW regions, is in agreement with region studies on  $ET_{pan}/ET_0$  by Liu and Zhang (2012)<sup>37</sup> and Li *et al.*<sup>24</sup>. When other sub-regions are considered, coarse periodic behaviors of  $ET_0$  change with two/or three turning point seems to be reasonable as compared with total decreasing-increasing patterns of evaporation in entire China reported by Cong *et al.*<sup>38</sup> and Liu *et al.*<sup>23</sup>. The combined effects of climatic variables to  $ET_0$  changes are revealed in all the sub-regions with the sensitive analysis, and are effective with a good agreement between the observed and calculated  $ET_0$  trends (see Table S2). Although relative humidity is the most sensitive variable (followed by net radiation, wind speed and air temperature) for all the period as well as all the sub-regions except SW and TP region, there are different dominating factors for  $ET_0$  change because the contributions of climate factors depend on the combined effect between sensitivity and trends of a variable itself<sup>9</sup>. Decline of net radiation only plays the important role for the  $ET_0$  decrease before early 1990s rather than the entire term in EC, SE and SW regions located in south China, highlighting the potential implications of “global dimming” in China over a roughly 1960–1990 period and a recovery (coined with “global brightening”) thereafter<sup>39,40</sup>, which is consistent with previous studies in China<sup>13,20,23,38,41</sup>, the United States<sup>3</sup>, the northeast of India<sup>42</sup>, and Greece<sup>43</sup>. There is consensus among many researchers that cloud coverage and aerosol, which are not completely independent variables with interaction in various ways<sup>44</sup>, are considered as the most likely candidates for the explanation of global dimming and brightening<sup>39,45–48</sup>. Particularly strong evidence for aerosol effects on surface solar radiation with increasing air pollution in China were noted in various studies<sup>49–52</sup>. As far as the other regions with larger inter-annual variability in  $ET_0$  are concerned, variation of wind speed generally plays more decisive role in the change of  $ET_0$  from 1961 to early 1990s, in line with the evidences reported in many places and summarized by McVicar *et al.*<sup>11</sup>. Although the dynamic mechanism of recent slow-down in near-surface global winds is complicated, it can generally be attributed to the increases of terrestrial surface roughness<sup>53,54</sup> or large scale atmospheric circulations<sup>55–58</sup>. Focusing on the periods after 1990s, our preliminary analyses have shown that dominating factors for the increases of  $ET_0$  transitioned from net radiation and wind speed to relative humidity for all the sub-regions. This coincides with the recent regional study in the arid regions of northwest china by Li *et al.*<sup>24</sup> and national wide study in China by Cong *et al.*<sup>38</sup>. A global evidence of reduction in surface atmospheric humidity revealed in this study in national scale was presented by Simmons *et al.*<sup>59</sup>. They inferred the recent reduction in relative humidity over land may be due to limited moisture supply from the oceans. For the purpose of simplification, the systemic errors of contribution analysis reflected by the differences between observed  $ET_0$  and compiled trends may be due to the interactions among climatic factors (which were not considered here but may exist in practice) and ignorance of other factors such as aerosol and dust.

From global perspective, there is an indication for a shift that occurred in the late 1970s with minor change occurred around 1990 and 2000 for PDO<sup>60,61</sup>. Having the strong correlation with PDO, the decadal variations of

$ET_0$  in China with two turning points during 1961–2011 are likely dominated by the episodic dynamics of climatic system, indicating that the recent  $ET_0$  trends in China reflect PDO conditions and are not the consequence of a persistent reorganization of the hydro-meteorological cycle. The similar conclusions have also been obtained from the global analysis for continental evaporation<sup>27,28</sup>. Consequently, the widely reported “evaporation paradox”, a counterintuitive behavior, representing that evapotranspiration decrease despite the increase of air temperature, seem to be more reasonably explained as part of a climate oscillation, at least in China<sup>33</sup>. The emerging picture of enhanced of  $ET_0$  in southern China highlights the possible threat posed by acceleration of the terrestrial hydrological cycle to water resources management and food security in an enhanced-greenhouse-affected climate.

## Materials and Methods

**Data.** Daily measurements of air temperatures (minimum, maximum and average) at 2 m height, relative humidity, wind speed at 10 m height, and sunshine duration obtained from the National Climatic Centre (NCC) for 602 ground-based stations in China during the period 1961–2011, provided by the National Meteorological Information Centre of China (NMIC) of the China Meteorological Administration (CMA), are used for estimating  $ET_0$  by Penman-Montieth method. Wherein, wind speed was adjusted to 2 m height by virtue of wind profile relationship proposed by Allen *et al.*<sup>62</sup>. Net radiation at 51 stations was available. Moreover, precipitation data from these meteorological stations were also collected.

**Food and Agriculture Organization (FAO) Penman-Montieth (P-M) Method.** From the reference surface defined as “a hypothetical reference grass with an assumed crop height of 0.12 m, a fixed surface resistance of 70 s m<sup>-1</sup> and an albedo of 0.23”, the daily reference evapotranspiration ( $ET_0$ ) is estimated by the Penman-Montieth (P-M) combination method, which is recommended by the FAO as a standard to calculate  $ET_0$  wherever the required input data are available and is proven to have good performance for various climatic conditions worldwide<sup>9</sup>. The P-M equation can be expressed as (Allen *et al.*)<sup>62</sup>:

$$ET_0 = \frac{0.408\Delta(R_n - G) + \gamma(900/(T + 273))u_2(e_s - e_a)}{\Delta + \gamma(1 + 0.34u_2)} \quad (1)$$

where  $ET_0$  is the reference evapotranspiration (mmd<sup>-1</sup>),  $R_n$  is the net radiation at the crop surface (MJ m<sup>-2</sup> d<sup>-1</sup>),  $G$  is the soil heat flux density (MJ m<sup>-2</sup> d<sup>-1</sup>),  $T$  is the mean daily air temperature (°C),  $u_2$  is the daily average wind speed at 2 m above ground level (ms<sup>-1</sup>),  $e_s$  is the saturation vapor pressure (kPa),  $e_a$  is the actual vapor pressure (kPa),  $e_s - e_a$  is the saturation vapor pressure deficit (kPa),  $\Delta$  is the slope of the saturated vapor pressure in relation to air temperature (kPa °C<sup>-1</sup>) and  $\gamma$  is the psychrometric constant (kPa °C<sup>-1</sup>).

As the difference between incoming net shortwave radiation ( $R_{ns}$ ) and outgoing net longwave radiation ( $R_{nl}$ ),  $R_n$  can be expressed as:

$$R_n = R_{ns} - R_{nl} \quad (2)$$

$R_{ns}$  is derived from the balance between incoming and reflected solar radiation and is given by:

$$R_{ns} = (1 - \alpha)R_s \quad (3)$$

where  $\alpha$  is the albedo or canopy reflection coefficient, which is 0.23 for the hypothetical grass reference crop.

$R_s$  can be estimated from sunshine duration (or hours of sunshine) with the help of the Angstrom formula

$$R_s = \left( a_s + b_s \frac{n}{N} \right) R_a \quad (4)$$

where  $R_s$  is the solar or shortwave radiation (MJ m<sup>-2</sup> d<sup>-1</sup>),  $n$  is the actual duration of sunshine (h),  $N$  is the maximum possible duration of sunshine or daylight hours (h), ( $\frac{n}{N}$  is thus the relative sunshine duration),  $R_a$  is the extraterrestrial radiation (MJ m<sup>-2</sup> d<sup>-1</sup>),  $a_s$  and  $b_s$  are the Angstrom coefficients. We calibrate the Angstrom coefficient using the observation of  $n$  and  $R_s$  from 51 stations widespread the whole China. Meanwhile,  $R_a$  and  $N$  are computed based on date and latitude according to the equations provided by the FAO P-M method. Overall, the high  $R^2$  values (see Table S3) between observed and estimated  $R_s$  indicate that the Angstrom model is suitable for daily global radiation estimation in China. For stations with no observation of solar radiation but sunshine duration,  $a_s$  and  $b_s$  are estimated by Kringing interpolation method.

$R_{nl}$  is based on water vapor, clouds, carbon dioxide and dust are absorbers and emitters of longwave radiation, and can be estimated by

$$R_{nl} = 2.45 \times 10^{-9} \cdot (0.9n/N + 0.1) \cdot (0.34 - 0.14\sqrt{e_a}) \cdot (T_{max,K}^4 + T_{min,K}^4) \quad (5)$$

where  $T_{max,K}$  and  $T_{min,K}$  are respectively maximum and minimum absolute temperatures during the 24-hour period,  $K = °C + 273.16$ .

The soil heat flux,  $G$ , is the energy that is utilized in heating the soil.  $G$  is positive when the soil is warming and negative when the soil is cooling. The soil heat flux is small compared to  $R_n$  and may often be ignored in daily evapotranspiration estimating.

**Trend analysis and breakpoint identification.** A simple linear regression method was used to calculate the slope of linear least squares regression line fit to the inter-annual variation of  $ET_0$  and other climatic

variables inputted in the P-M equation. The significance of changes of these variables across China was mapped and assessed with the help of the two-tailed significance tests. The segmented regression with constraints method developed by Shao and Campbell<sup>63</sup>, which can detect both shift trends and step changes simultaneously without knowing the number of trend segments and change points and their location over time<sup>64</sup>, is employed to investigate the possible turning points of the regional average  $ET_0$  series across China. The method was summarily described as follow<sup>63-65</sup>:

Assuming that  $x_i$  means the observed variable at time  $t_i$  ( $i = 1, 2, \dots, N$ ), the regression can be written as

$$x_i = u(t_i) + \varepsilon_i \quad (i = 1, 2, \dots, N) \quad (6)$$

where the errors  $\{\varepsilon_i\}$  ( $i = 1, 2, \dots, N$ ) are assumed to be independent and identically distributed as  $N(0, \sigma^2)$ . For  $L$  abrupt change points  $r_1 < r_2 < \dots < r_L$ , resulting in  $L + 1$  segments, the model can be written as

$$u(t) = u_l(t) \quad r_{l-1} < t < r_l \quad (l = 1, 2, \dots, L + 1) \quad (7)$$

with  $r_0 = 0$ ,  $r_{L+1} = \infty$  and  $u_l(t)$  are the deterministic part quantifying the trends. Suppose that there are  $j_l$  join points  $\{J_{l,k}\}$  ( $k = 1, 2, \dots, j_l$ ) in the  $l$ th segment between the break points  $r_{l-1}$  and  $r_l$ ,  $u_l(t)$  can be defined as:

$$u_l(t) = a_l + \sum_{k=1}^{j_l} b_{l,k}(t - J_{l,k})_+ \quad (l = 1, 2, \dots, L + 1) \quad (8)$$

with  $J_{l,0} = r_{l-1}$ , where  $(t - J_{l,k})_+ = u_+$  is defined as  $u_+ = u$  if  $u \geq 0$ . A modified Akaike's information criterion (AICc), derived by Hurvich and Tasi<sup>66</sup> with  $c$  standing for the second order correction<sup>67</sup>, is employed to select an optimal numbers of break and join points and their locations, and the optimal model can be obtained by minimizing AICc.

**The Rotated Empirical Orthogonal Function (REOF) method.** To characterize in detail the spatial variability of  $ET_0$  at nationwide scale and identify the homogenous regions, we applied REOF to analyze the most dominant spatial patterns. The aim of the EOF method is to find a relatively small number of independent variables conveying as much of the original information as possible without redundancy by decomposing a multivariate data set into uncorrelated linear combination of separate function of the original variables. However, the physical interpretability of the obtained patterns is sometimes a matter of controversy because of orthogonality in both space and time<sup>68</sup>. This limitation has brought about the development of the rotated empirical orthogonal function (REOF)<sup>69</sup>, which can cluster within each mode a small number of high valued variables and a large number of near-zero value variables through a rotation to simple structure. In a comparison study by Kim and Wu<sup>70</sup>, REOF was found to be better in dividing climatic patterns. In this paper, with maximizing the variance of the squared correlation between each rotated principal component (RPCs) and each variable, the varimax REOF method was chosen to give the simplest pattern description while explaining the maximum amount of variance.

**The differentiation equation method.** For the function  $y = f(x_1, x_2, \dots)$ , the variation of the dependent variable  $y$  over the time  $t$  can be mathematically written by a differential equation as

$$\frac{dy}{dt} = \sum \frac{\partial f}{\partial x_i} \frac{dx_i}{dt} = \sum f'_i \frac{dx_i}{dt} \quad (9)$$

where  $x_i$  is the  $i$ th independent variable and  $f'_i = \frac{\partial f}{\partial x_i}$

Assuming that  $y$  and  $x_i$  are the time series variables,  $\frac{dy}{dt}$  and  $\frac{dx_i}{dt}$  should be the long-term trend for  $y$  and  $x_i$ , respectively. The term of  $f'_i \frac{dx_i}{dt}$ , the product of long-term change in  $x_i$  and the partial derivative, can then be considered as the contribution of change in  $x_i$  to the long-term variation of  $y$ . Thus, following P-M equation for  $ET_0$  estimation, contributions of changes in key climatic factors to  $ET_0$  variation can be approximately as<sup>55</sup>:

$$\frac{dET_0}{dt} = \frac{\partial ET_0}{\partial R_n} \frac{dR_n}{dt} + \frac{\partial ET_0}{\partial T} \frac{dT}{dt} + \frac{\partial ET_0}{\partial U} \frac{dU}{dt} + \frac{\partial ET_0}{\partial RH} \frac{dRH}{dt} + \delta \quad (10)$$

where  $\frac{dET_0}{dt}$  is the long-term change in  $ET_0$  estimated by the above partial derivatives.  $\frac{\partial ET_0}{\partial R_n} \frac{dR_n}{dt}$ ,  $\frac{\partial ET_0}{\partial T} \frac{dT}{dt}$ ,  $\frac{\partial ET_0}{\partial U} \frac{dU}{dt}$  and  $\frac{\partial ET_0}{\partial RH} \frac{dRH}{dt}$  are respectively the contributions to the long-term change in  $ET_0$  due to the variation in  $R_n$ ,  $T$ ,  $U$  and  $RH$ .  $\delta$  is the error term.

**The sensitive coefficient.** For such a multi-variable model of P-M equation, it is difficult to compare the sensitivity by partial derivatives due to the different dimensions and ranges of values for related variables. Hence, the partial derivative is transformed into a non-dimensional form in term of McCuen<sup>71</sup> and Beven<sup>72</sup> to express the sensitivity of the climatic variables mathematically:

$$S(x_i) = \lim_{\Delta x_i \rightarrow 0} \left( \frac{\Delta ET_0 / ET_0}{\Delta x_i / x_i} \right) = \frac{\partial ET_0}{\partial x_i} \cdot \frac{x_i}{ET_0} \quad (11)$$

where  $S(x_i)$  is the sensitivity coefficient of  $ET_0$  related to  $x_i$ , the  $i$ th variable. Being first employed by McCuen<sup>71</sup>, the sensitivity coefficient has been widely used in evaluating the climatic response of evapotranspiration, especially during recent two decades<sup>73–77</sup>.

## References

- Xu, C. Y. & Singh, V. P. Evaluation of three complementary relationship evapotranspiration models by water balance approach to estimate actual regional evapotranspiration in different climatic regions. *J Hydrol* **308**, 105–121 (2005).
- Zhang, Y., Liu, C., Tang, Y. & Yang, Y. Trends in pan evaporation and reference and actual evapotranspiration across the Tibetan Plateau. *J Geophys Res* **112**, D12110, doi: 10.1029/2006JD008161 (2007).
- Peterson, T. C., Golubev, V. S. & Groisman, P. Y. Evaporation losing its strength. *Nature* **377**, 687–688 (1995).
- Roderick, M. L. & Farquhar, G. D. The cause of decreased pan evaporation over the past 50 years. *Science* **298**, 1410–1411 (2002).
- Brutsaert, W. & Parlange, M. Hydrologic cycle explains the evaporation paradox. *Nature* **396**, 30 (1998).
- Linacre, E. T. Evaporation trends. *Theor Appl Climatol* **79**, 11–21 (2004).
- Ramírez, J. A., Hobbins, M. T. & Brown, T. C. Observational evidence of the complementary relationship in regional evaporation lends strong support for Bouchet's hypothesis. *Geophys Res Lett* **32**, L15401, doi: 10.1029/2005GL023549 (2005).
- Roderick, M. L., Hobbins, M. T. & Farquhar, G. D. Pan evaporation trends and the terrestrial water balance. I. Principles and observations. *Geogr Campass* **3**, 746–760 (2009).
- Wang, W. *et al.* Reference evapotranspiration change and the causes across the Yellow River Basin during 1957–2008 and their spatial and seasonal differences. *Water Resour Res* **48**, W05530, doi: 10.1029/2011WR010724 (2012).
- Roderick, M. L., Rotstain, L. D., Farquhar, G. D. & Hobbins, M. T. On the attribution of changing pan evaporation. *Geophys Res Lett* **34**, L17403, doi: 10.1029/2007GL031166 (2007).
- McVicar, T. R. *et al.* Global review and synthesis of trends in observed terrestrial near-surface wind speeds: Implications for evaporation. *J Hydrol* **416–417**, 182–205 (2012).
- Thomas, A. Spatial and temporal characteristics of potential evapotranspiration trends over China. *J Climatol* **20**, 381–396 (2000).
- Liu, B., Xu, M., Henderson, M. & Gong, W. A spatial analysis of pan evaporation trends in China, 1955–2000. *J Geophys Res* **109**, D15102, doi: 10.1029/2004JD004511 (2004).
- Gao, G., Chen, D. L., Ren, G. Y., Chen, Y. & Liao, Y. M. Spatial and temporal variations and controlling factors of potential evapotranspiration in China: 1956 to 2000. *J Geogr Sci* **16**, 3–12 (2006).
- Cong, Z. & Yang, D. Does evaporation paradox exist in China? *Hydrol Earth Syst Sci* **13**, 357–366 (2009).
- Wang, W. *et al.* Spatial and temporal characteristics of reference evapotranspiration trends in the Haihe River basin, China. *J Hydrol Eng* **16**, 239–252 (2011).
- Huo, Z., Dai, X., Feng, S., Kang, S. & Huang, G. Effect of climate change on reference evapotranspiration and aridity index in arid region of China. *J Hydrol* **492**, 24–34, doi: 10.1016/j.jhydrol.2013.04.011 (2013).
- Zheng, C. & Wang, Q. Spatiotemporal variations of reference evapotranspiration in recent five decades in the arid land of Northwestern China. *Hydrol Process* **28**, 6124–6134, doi: 10.1002/hyp.10109 (2014).
- Zhang, K. *et al.* Influence of climate change on reference evapotranspiration and aridity index and their temporal-spatial variations in the Yellow River Basin, China, from 1961 to 2012. *Quat Int* **380–381**, 75–82 (2015).
- Xu, C. Y., Gong, L., Jiang, T., Chen, D. & Singh, V. P. Analysis of spatial distribution and temporal trend of reference evapotranspiration and pan evaporation in Changjiang (Yangtze River) catchment. *J Hydrol* **327**, 81–93 (2006).
- Zhang, X., Ren, Y., Yin, Z. Y., Lin, Z. & Zheng, D. Spatial and temporal variation patterns of reference evapotranspiration across the Qinghai-Tibetan Plateau during 1971–2004. *J Geophys Res* **114**, D15105, doi: 10.1029/2009JD011753 (2009).
- Yin, Y., Wu, S., Chen, G. & Dai, E. Attribution analyses of potential evapotranspiration changes in China since the 1960s. *Theor Appl Climatol* **101**, 19–28 (2010).
- Liu, X., Luo, Y., Zhang, D., Zhang, M. & Liu, C. Recent changes in pan-evaporation dynamics in China. *Geophys Res Lett* **38**, L13404, doi: 10.1029/2011GL047929 (2011).
- Li, Z. *et al.* Analysis of changing pan evaporation in the arid region of Northwest China. *Water Resour Res* **49**, 2205–2212, doi: 10.1002/wrcr.20202 (2013).
- Wang, W. *et al.* Changes in reference evapotranspiration across the Tibetan Plateau: Observations and future projections based on statistical downscaling. *J Geophys Res* **118**, 1–20 (2013).
- Jung, M. *et al.* Recent decline in the global land evapotranspiration trend due to limited moisture supply. *Nature* **467**, 951–954, doi: 10.1038/nature09396 (2010).
- Miralles, D. G. *et al.* El Niño-La Niña cycle and recent trends in continental evaporation. *Nat Clim Change* **4**, 122–126 (2014).
- Zhang, K. *et al.* Vegetation Greening and Climate Change Promote Multidecadal Rises of Global Land Evapotranspiration. *Scientific Reports* **5**, 15956, doi: 10.1038/srep15956 (2015).
- Bouchet, R. J. Evapotranspiration réelle et potentielle, signification climatique. *IAHS Publ* **62**, 134–142 (1963).
- Ma, Z. The interdecadal trend and shift of dry/wet over the central part of north China and their relationship to the Pacific decadal oscillation (PDO). *Chin Sci Bull* **52**, 2130–2139 (2007).
- Li, H., Dai, A., Zhou, T. & Lu, J. Responses of East Asian summer monsoon to historical SST and atmospheric forcing during 1950–2000. *Climate Dyn* **34**, 501–514 (2010).
- Qian, C. & Zhou, T. Multidecadal variability of North China aridity and its relationship to PDO during 1900–2010. *J Clim* **27**, 1210–1222 (2014).
- Yu, L., Furevik, T., Otterå, O. H. & Gao, Y. Q. Modulation of the Pacific Decadal Oscillation on the summer precipitation over East China: A comparison of observations to 600-years control run of Bergen Climate Model. *Climate Dyn* **44**, 475–494 (2015).
- Huang, H. *et al.* Spatiotemporal Characteristics of Evapotranspiration Paradox and Impact Factors in China in the Period of 1960–2013. *Adv Meteorol* **2015(4)**, 1–10, doi: 10.1155/2015/519207 (2015).
- Lu, X., Bai, H. & Mu, X. Explaining the evaporation paradox in Jiangxi Province of China: Spatial distribution and temporal trends in potential evapotranspiration of Jiangxi Province from 1961 to 2013. *Int Soil & Water Conserv Res* **4**, 45–51 (2016).
- Fan, J., Wu, L., Zhang, F., Xiang, Y. & Zheng, J. Climate change effects on reference crop evapotranspiration across different climatic zones of China during 1956–2015. *J Hydrol* doi: 10.1016/j.jhydrol.2016.09.060 (2016).
- Liu, X. & Zhang, D. Trend analysis of reference evapotranspiration in Northwest China: the roles of changing wind speed and surface air temperature. *Hydrol Process* **27**, 3941–3948 (2013).
- Cong, Z., Yang, D., Gao, B., Yang, H. & Hu, H. Hydrological trend analysis in the Yellow River basin using a distributed hydrological model. *Water Resour Res* **45**, W00A13, doi: 10.1029/2008WR006852 (2009).
- Wild, M. *et al.* Global dimming and brightening: An update beyond 2000. *J Geophys Res* **114**, D00D13, doi: 10.1029/2008JD011382 (2009).
- Qian, Y. *et al.* More frequent cloud-free sky and less surface solar radiation in China from 1955 to 2000. *Geophys Res Lett* **33**, L01812, doi: 10.1029/2005GL024586 (2006).
- Liu, Q., Yang, Z., Cui, B. & Sun, T. The temporal trends of reference evapotranspiration and its sensitivity to key meteorological variables in the Yellow River Basin, China. *Hydrol Processes* **24**, 2171–2181 (2010).

42. Jhajharia, D., Shrivastava, S. K., Sarkar, D. & Sarkar, S. Temporal characteristics of pan evaporation trends under the humid conditions of northeast India. *Agric For Meteorol* **149**, 763–777 (2009).
43. Papaioannou, G., Kitsara, G. & Athanasatos, A. Impact of global dimming and brightening on reference evapotranspiration in Greece. *J Geophys Res* **116**, D09107, doi: 10.1029/2010JD015525 (2011).
44. Ramanathan, V., Crutzen, P. J., Kiehl, J. T. & Rosenfeld, D. Atmosphere—aerosols, climate, and the hydrological cycle. *Science* **294**, 2119–2124 (2001).
45. Liepert, B. G. Recent changes in solar radiation under cloudy conditions in Germany. *Int J Climatol* **17**, 1581–1593, doi: 10.1002/(SICI)1097-0088 (1997).
46. Liley, B. New Zealand dimming and brightening. *J Geophys Res* **114**, D00D10, doi: 10.1029/2008JD011401 (2009).
47. Ramanathan, V. *et al.* Warming trends in Asia amplified by brown cloud solar absorption. *Nature* **448**, 575–578 (2007).
48. Wild, M. *et al.* From dimming to brightening: Decadal changes in solar radiation at Earth's surface. *Science* **308**, 847–850 (2005).
49. Zhang, Y., Qin, B. & Chen, W. Analysis of 40 year records of solar radiation data in Shanghai, Nanjing and Hangzhou in Eastern China. *Theor Appl Climatol* **78**, 217–227 (2004).
50. Xia, X., Wang, P., Chen, H. & Liang, F. Analysis of downwelling surface solar radiation in China from National Center for Environmental Prediction reanalysis, satellite estimates, and surface observations. *J Geophys Res* **111**, D09103, doi: 10.1029/2005JD006405 (2006).
51. Qian, Y., Wang, W., Leung, L. R. & Kaiser, D. P. Variability of solar radiation under cloud-free skies in China: The role of aerosols. *Geophys Res Lett* **34**, L12804, doi: 10.1029/2006GL028800 (2007).
52. Shi, G. *et al.* Data quality assessment and the long-term trend of ground solar radiation in China. *J Appl Meteorol Climatol* **47**, 1006–1016, doi: 10.1175/2007JAMC1493.1 (2008).
53. Bandyopadhyay, A., Bhadra, A., Raghuvanshi, N. S. & Singh, R. Temporal trends in estimates of reference evapotranspiration over India. *J Hydrol Eng* **14**, 508–515 (2009).
54. Vautard, R., Gattiaux, J., Yiou, P., The'paut, J. N. & Ciais, P. Northern Hemisphere atmospheric stilling partly attributed to increased surface roughness. *Nature Geosci* **3**, 756–761 (2010).
55. Zheng, H., Liu, M., Liu, C., Dai, X. & Zhu, R. Assessing contributions to pan evaporation trends in Haihe River Basin, China. *J Geophys Res* **114**, D24105, doi: 10.1029/2009JD012203 (2009).
56. Rayner, D. P. Wind run changes: the dominant factor affecting pan evaporation trends in Australia. *J Clim* **20**, 3379–3394 (2007).
57. Jiang, Y., Luo, Y., Zhao, Z. & Tao, S. Changes in wind speed over China during 1956–2004. *Theor Appl Climatol* **99**, 421–430 (2010).
58. Brutsaert, W. Global land surface evaporation trend during the past half century: Corroboration by Clausius-Clapeyron scaling. *Adv Water Resour* doi: 10.1016/j.advwatres.2016.08.014 (2016).
59. Simmons, A. J., Willett, K. M., Jones, P. D., Thorne, P. W. & Dee, D. Low-frequency variations in surface atmospheric humidity, temperature and precipitation: Inferences from reanalyses and monthly gridded observational datasets. *J Geophys Res* **115**, D011110, doi: 10.1029/2009JD012442 (2010).
60. Minobe, S. Resonance in bidecadal and pentadecadal climate oscillations over the North Pacific: Role in climatic regime shifts. *Geophys Res Lett* **26**, 855–858 (1999).
61. Chiacchio, M. & Wild, M. Influence of NAO and clouds on long term seasonal variations of surface solar radiation in Europe. *J Geophys Res* **115**, D00D22, doi: 10.1029/2009JD012182 (2010).
62. Allen, R. G., Pereira, L. S., Raes, D. & Smith, M. *Crop evapotranspiration—Guidelines for computing crop water requirements*. FAO Irrigation and Drainage Paper 56, Food and Agriculture Organization of the United Nations, Rome, Italy (1998).
63. Shao, Q. & Campbell, N. A. Modeling trends in groundwater levels by segmented regression with constraints. *Australian & New Zealand J Statist* **44**, 129–141 (2002).
64. Shao, Q., Li, Z. & Xu, Z. Trend detection in hydrological time series by segment regression with application to Shiyang River Basin. *Stoch Environ Res Risk Assess* **24**, 221–233 (2010).
65. Wang, W. *et al.* Spatial and temporal characteristics of changes in precipitation during 1957–2007 in the Haihe River basin, China. *Stoch Environ Res Risk Assess* **25**, 881–895 (2011).
66. Hurvich, M. & Tsai, C. L. Regression and time series model selection in small samples. *Biometrika* **76**, 297–307 (1989).
67. McQuaarie, A. D. R. & Tsai, C. L. *Regression and Time Series Model Selection* pp. 24–34, World Scientific, Singapore (1998).
68. Su, B., Gemmer, M. & Jiang, T. Spatial and temporal variation of extreme precipitation over the Yangtze River Basin. *Quatern Int* **186**, 22–31 (2008).
69. Richman, M. B. Rotation of principal components. *J Climatol* **6**, 293–335 (1986).
70. Kim, K. Y. & Wu, Q. A comparison study of EOF techniques: Analysis of nonstationary data with periodic statistic. *J Clim* **12**, 185–199 (1999).
71. McCuen, R. H. A sensitivity and error analysis of procedures used for estimating evaporation. *Water Resour Bull* **10**, 486–498 (1974).
72. Beven, K. A sensitivity analysis of the Penman-Monteith actual evapotranspiration estimates. *J Hydrol* **44**, 169–190, doi: 10.1016/0022-1694(79)90130-6 (1979).
73. Qiu, G., Yanob, T. & Momiic, K. An improved methodology to measure evaporation from bare soil based on comparison of surface temperature with a dry soil surface. *J Hydrol* **210**, 93–105, doi: 10.1016/S0022-1694(98)00174-7 (1998).
74. Rana, G. & Katerji, N. A measurement based sensitivity analysis of the Penman-Monteith actual evapotranspiration model for crops of different height and in contrasting water status. *Theor Appl Climatol* **60**, 141–149, doi: 10.1007/s007040050039 (1998).
75. Hupet, F. & Vanclooster, M. Effect of the sampling frequency of meteorological variables on the estimation of the reference evapotranspiration. *J Hydrol* **243**, 192–204, doi: 10.1016/S0022-1694(00)00413-3 (2001).
76. Gong, L., Xu, C. Y., Chen, D., Halldin, S. & Chen, Y. Sensitivity of the Penman-Monteith reference evapotranspiration to key climatic variables in Changjiang (Yangtze River) Basin. *J Hydrol* **329**, 620–629, doi: 10.1016/j.jhydrol.2006.03.027 (2006).
77. Yang, H. & Yang, D. Climatic factors influencing changing pan evaporation across China from 1961 to 2001. *J Hydrol* **414–415**, 184–193 (2012).

## Acknowledgements

This work was jointly supported by the National Science Foundation of China (51379057), the Fundamental Research Funds for the Central Universities (2015B14114), the National “Ten Thousand Program” Youth Talent, and the QingLan Project.

## Author Contributions

W.W. designed the research and wrote the manuscript; W.X. collected the data and conducted the data analysis; W.W., W.X., Q.S., Z.Y., T.Y. and J.F. discussed the results, and commented on the manuscript.

## Additional Information

**Supplementary information** accompanies this paper at <http://www.nature.com/srep>

**Competing financial interests:** The authors declare no competing financial interests.

**How to cite this article:** Xing, W. *et al.* Periodic fluctuation of reference evapotranspiration during the past five decades: Does Evaporation Paradox really exist in China? *Sci. Rep.* **6**, 39503; doi: 10.1038/srep39503 (2016).

**Publisher's note:** Springer Nature remains neutral with regard to jurisdictional claims in published maps and institutional affiliations.



This work is licensed under a Creative Commons Attribution 4.0 International License. The images or other third party material in this article are included in the article's Creative Commons license, unless indicated otherwise in the credit line; if the material is not included under the Creative Commons license, users will need to obtain permission from the license holder to reproduce the material. To view a copy of this license, visit <http://creativecommons.org/licenses/by/4.0/>

© The Author(s) 2016